Iraqi Journal of Natural Sciences and Nanotechnology IJNSN

Study the Effect of Anode on the Nanostructure of ZrO_2 Prepared by Atmospheric Pressure Plasma Jet Technique Used in Biological Application

Hiba Nabeel Abbas[1], Wasan H. Al-Husseny[2], Ahmed Abed Anber[3*]

[1]Department of Microbiology, College of Science, AL- Karkh University of Science, Baghdad, Iraq

[2] Department of Physics, College of Science, Mustansriryah University

[3] Department of Medical Physics, College of Science, AL- Karkh University of Science, Baghdad, Iraq

Corresponding Author : Ahmed.abed@kus.edu.iq

Keywords:

Atmospheric-pressure plasma jet technique; Anti-bacterial activity; ZrO2 nano-powders ;

Abstract

In this work, atmospheric pressure plasma jet system was designed and constructed to synthesis nanomaterials such as ZrO2 nanopowders. The system consist of many sections: Plasma Jet (syringe), high voltage (AC). power supply, regulator, magnetic stirrer and Argon gas. The preparation plan includes the effect of changing the an electrode (Anode) using Fe electrode piece and Ni electrode strip on the ZrO2 nanopowders. The bonds location for both prepared phases was determined by Fourier-transformation infrared (FT-IR) spectroscopy. ZrO2 nanostructures were highly pure and reasonably homogeneous. The average particle size was determined from FE-SEM. The antibacterial activity of ZrO2 nanoparticles have been obtained. It was impeccable inhibition zone after that 24 h. incubation at 37 oC in the plate. The strains predisposed to ZrO2 nanoparticles show a large inhibition zone, for two types of bacteria (S.arueas and E.coli).

Introduction

Zirconium dioxide is one of the most usually used in ceramic oxides materials. Its applications range from use in grainy products and dental crowns, and its most natural procedure in the mineral polishes. Moreover in cell membranes and in hip joints implants. It is the most commercially important oxide designed via Zr[1].

The applications of ZrO2 nanoparticles are highlighted. Electronics industries, Tools industrial and mechanical engineering the production of zirconium-based refractories, ceramics, glasses, solid materials and medical applications. The modification of ZrO2, stabilized via oxides of the rare earth, is a jewelry stone [2].

ZrO_2 nanoparticle is a upright conductivity of heat and electricity. The melting point and the boiling point around 1452 °C and 2913 °C respectively [3]. A thermal study by dried out samples verified delay in the crystallization structure of zirconia. When the an iron exist with the network content in the sample, add to more solidification of structure. The composition of the diverse phases have been demonstrated via numerous characterization. The reaction of Fe species with Zr was different according to preparation. A large scattering of the precipitated samples were detected [4,5,6]. The use of ceramic made of zirconia instead of aluminum casings improves the transmission of radio waves without the need to use an external antenna, but rather it is inside the device[7]. The process of cold atmospheric plasma jet configurations, needle-to-cylinder electrode configuration and single high-voltage electrode around the quartz tube. The APJs have been worked in argon gas flowing over a metal tube with 0.45 mm diameter into the ambient temperature, and the plasma was created by kHz frequency by ac power supply [8,9]. An importance study was on the mechanism of ionization wave for that configuration.

In this work the ZrO_2 nan powder was prepared by cold plasma as were the most widely studied. Kato et. al. [10-11] organized ZrO_2 by atmospheric pressure plasma. Other researchers [12] produced pure ZrO_2 precipitate by atmospheric dielectric barrier discharge plasma. Thermal plasma Compared with cold plasma methods seem to be more suitable to synthesize ZrO_2 photocatalysts because anatase phase has been reported to be more effective than rutile phase for photocatalysis [13-14]. In current years, several atmospheric pressure plasma jets have been advanced and characterized [15,16]. In contrast to other atmospheric pressure plasmas, the jet piece is not restricted via electrode and the dimension may be used to from a number of centimeters areas, leading to the grown treatment of surface. Furthermore, atmospheric pressure plasma jet can solve the compatibility of high plasma stability and effective reaction in atmospheric plasma. Subsequently exploding of plasma, the species produced in the jet are carried out to isolated area [17-20].

Experimental Setup

The system consist of anode and cathode, a voltage-controller, Argon gas tube, and a high tension power supply AC. Power source make up an atmospheric pressure plasma jet. This power source using to create the plasma jet in cold atmospheric plasmas. The power supply's output is 12 kV in the form of a sinusoidal wave, 2 mA, and 20 KHz, resulting in an AC. Figure (1) depicts the plasma jet system. The alternating current (AC) high voltage is used to operate the atmospheric plasma jet. This power supply provides variable A.C high voltage of range 0-12 kV, and frequency of range (0-20) kHz.

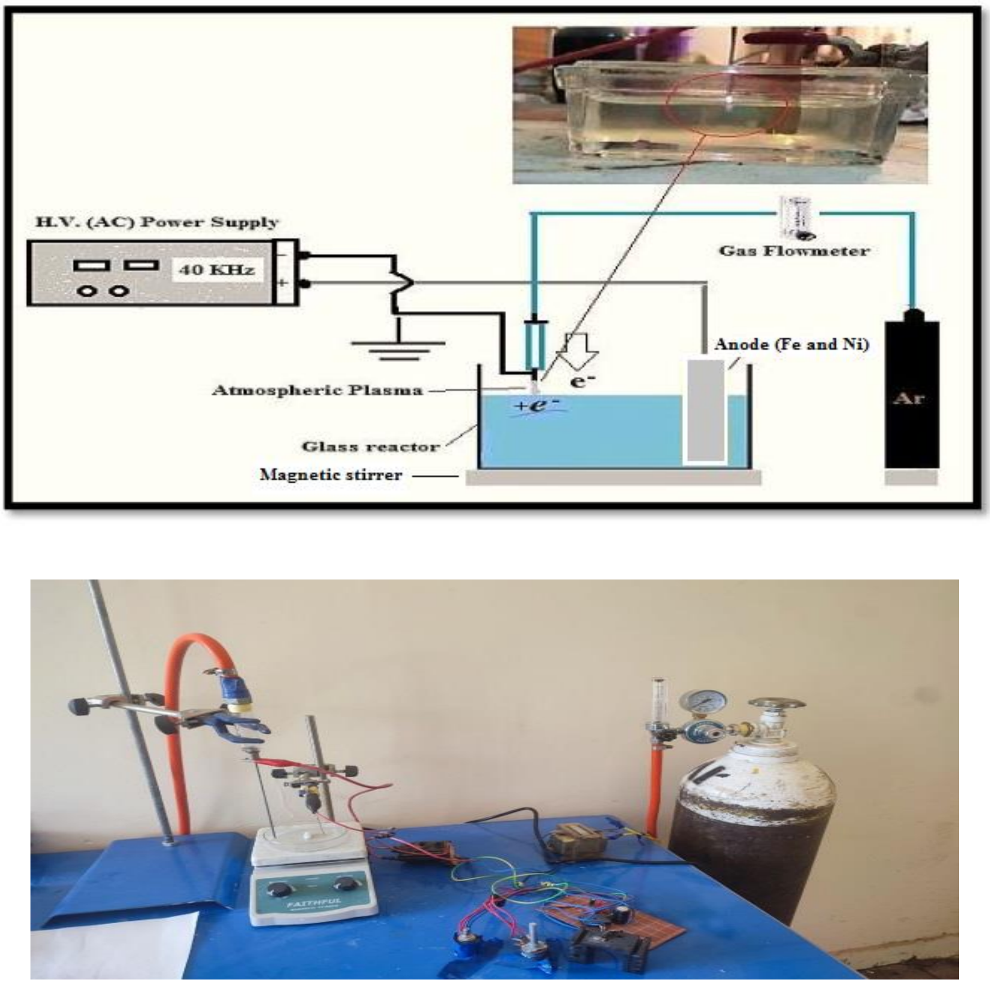

Figure 1The diagram of atmospheric plasma jet electrochemical production of ZrO2 nanopowder

Firstly for the nickel electrode. At a time of 30 minutes, 1.8 grams of zirconium and 0.2 grams of fructose were mixed with the addition of 5 milliliters of sulfuric acid at a pressure of 1 atm and 45 milliliters of water, taking into account the distance between the electrode and the cathode is 2 cm. As for the second model for the nickel electrode, at a time of 40 minutes, 1.8 grams of zirconium and 0.2 grams of fructose were mixed with the addition of 5 milliliters of sulfuric acid at a pressure of 1 atm and 45 milliliters of water, taking into account the distance between the electrode and the cathode is 2 cm. The second electrode is the iron electrode in the first model. At a time of 30 minutes, 1.8 grams/mol was mixed with 0.2 grams of fructose, 5 milliliters of sulfuric acid, and 45 milliliters of water at a pressure of 1 atm, and the distance between the iron electrode and the cathode is 2 cm. The second electrode is the iron electrode in the second model, at a time of 30 minutes, 1.8 grams/mol were mixed with 0.2 grams of fructose, 5 milliliters of sulfuric acid, and 45 milliliters of water at a pressure of 1 atm, and the distance between the iron electrode and the cathode was 2 cm.

Results and Discussion

Figure 2 and 3 display the FT-IR spectra of ZrO2 which displayed characteristics crests on around (725 cm^{-1} and 590 cm^{-1}), that resemble to the Zr-O stretching bond [21]. The spectrum displays that Fe-anode ZrO2 composition accomplished comparable FT-IR spectrum to clean ZrO2 nanoparticles [22]. It displayed two additional absorption peaks from place to place (1630 cm^{-1} and 3430 cm^{-1}), the characteristics peak at 3430 cm^{-1} indicates the stretching bond of OH due to the absorptions and water coordination, (Zr-OH). The band at 1630 cm^{-1} can be allocated to the water bending mode [21]. The Ni anode on ZrO2 nano-catalysts displayed like spectra to that of pure ZrO2 molecules.

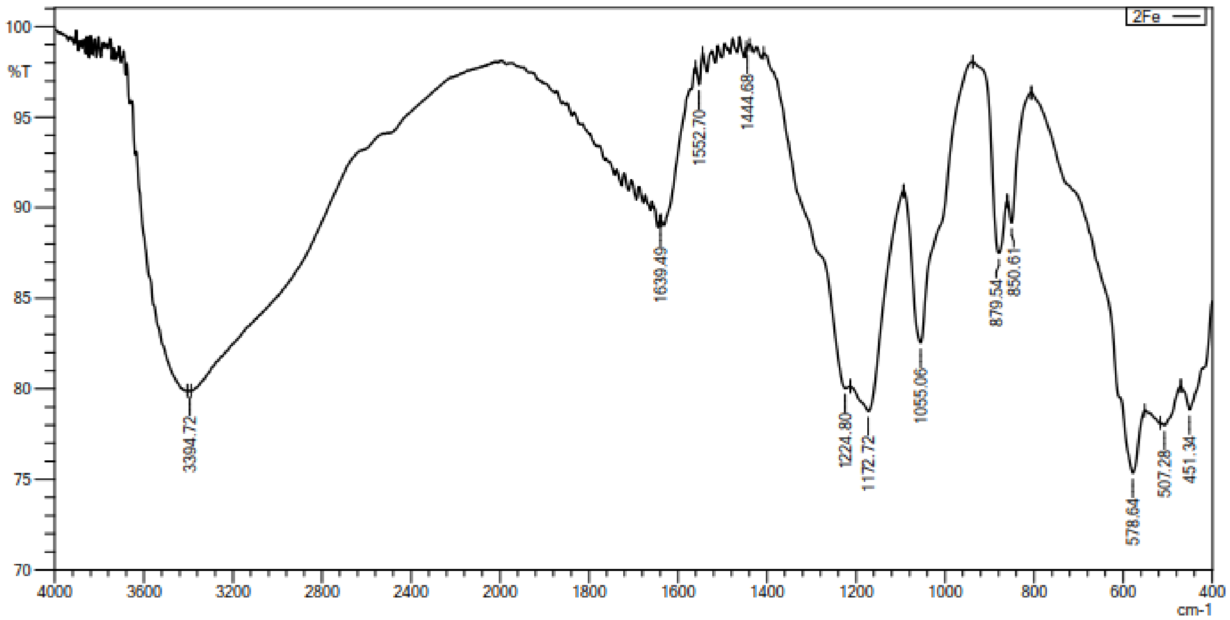

Figure 2 Illustrates the measurement of FTIR for prepared samples: ZrO2 with Fe anode prepared by an atmospheric-pressure plasma jet

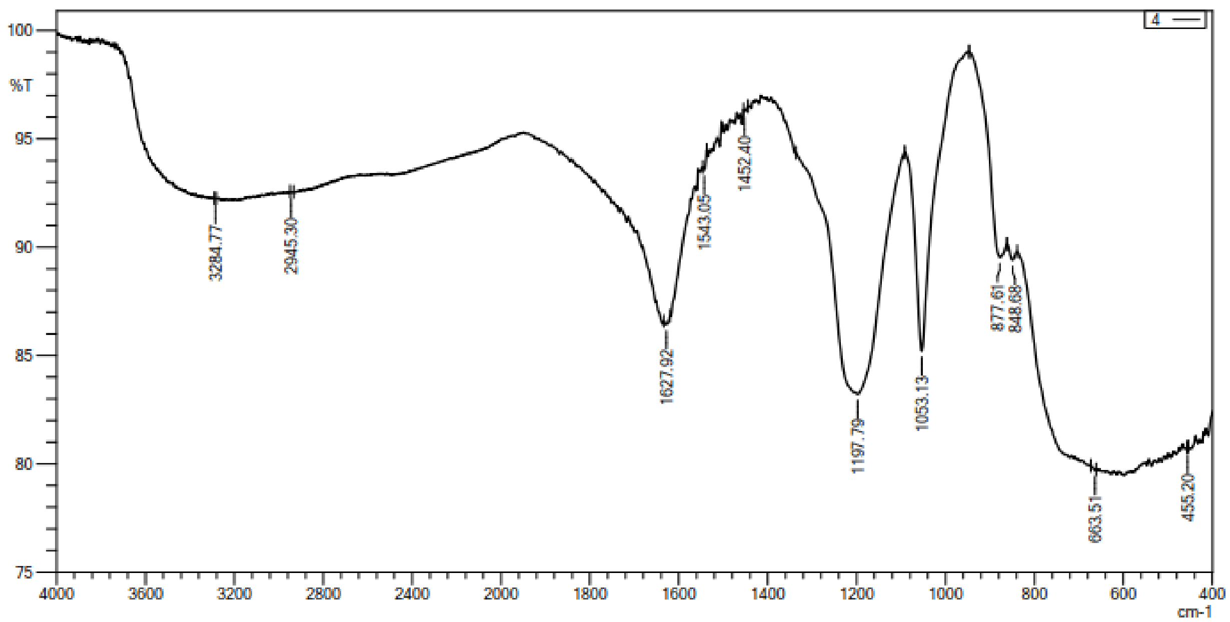

Figure 3 Illustrates the measurement of FTIR for prepared samples: ZrO2 with Ni anode prepared by atmospheric pressure plasma jet

Figure 4 and 5 show FE-SEM images, the high and low magnification field emission of ZrO2 with Fe and Ni anode respectively. From the figures it may show the ZrO2 contains particles of irregular distributions which are exceedingly porous. The nanoparticles form like structures and flakes are collected of interconnected pores of change size. The morphology of ZrO2 nanoparticles is stated earlier via Ramos-Bristo et al. [22]. Nevertheless, for difference in the surface morphology could be due to difference in the agglomeration of nanoparticles is representative of method synthesis. The size difference and numbers of void could be outstanding difference in changing types of anodes.

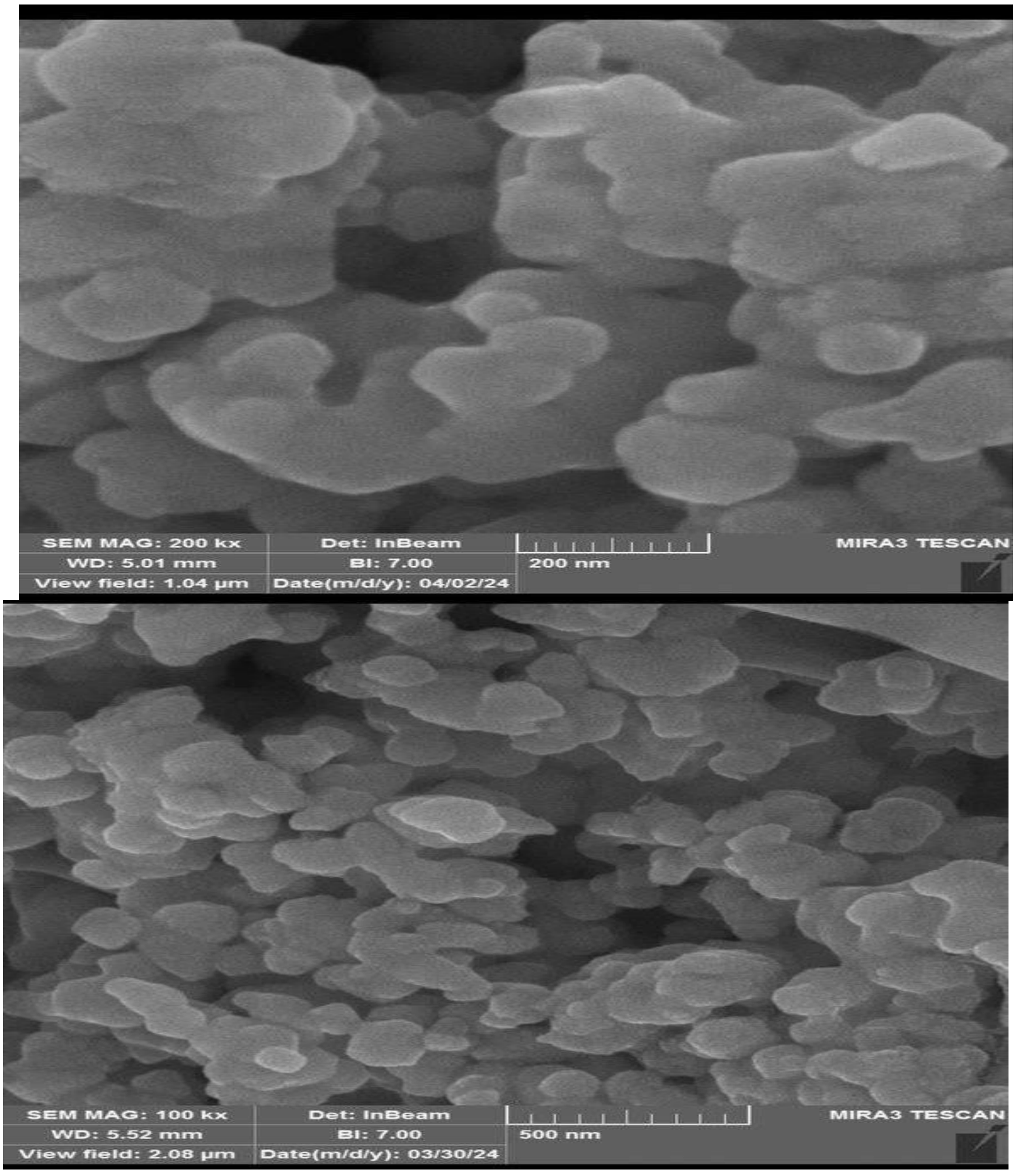

Figure 4 The SEM photo of ZrO2 with Fe anode prepared by atmospheric pressure plasma jet

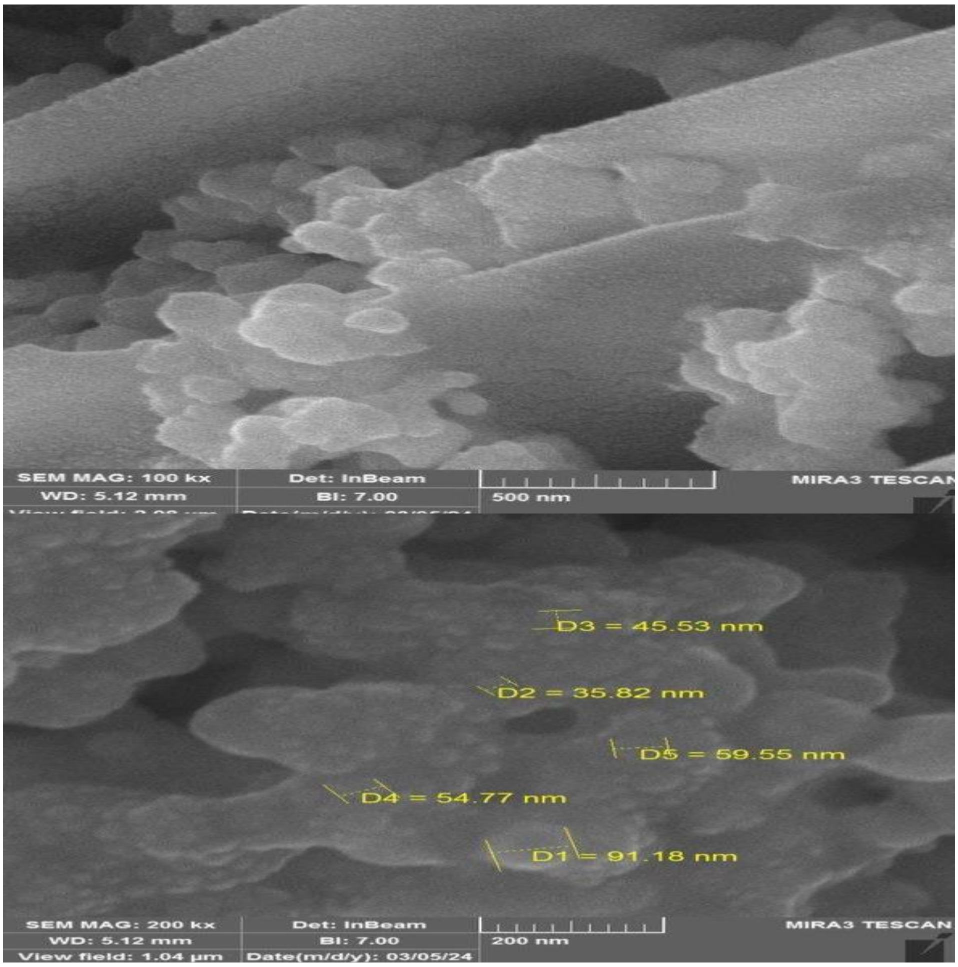

Figure 5 The SEM photo of ZrO2 with Ni anode prepared by atmospheric pressure plasma jet

The FE-SEM has been used to measure the nanoparticles size of all prepared samples. The results of this measurement deliver information about the effect of Fe anode content on the microstructure of the ZrO2 leads to increasing of grain size, These figures exposed that, in the sample that has no oxide content the grain boundaries have been minor and there was a groves making the surface of the prepared sample. Moreover, the several particles distributed among the surface which provide an indication to the aggregation process at these surfaces.

Figure (6 and 7) and Table (1) indicate that ZrO2 NPs have been displayed inhibiting effect to various kinds of bacteria. The activity of NPs compared to bacteria was described by numerous studies, but the mechanism of the bactericidal effect of nanoparticles is not agreed completely. But studies propose that when bacteria cured with ZrO2 nanoparticles. The nanoparticle attribute to surface of plasma membrane, then several changes took place in its membrane morphology and disturb its power function, produced a significant increase in its permeability affecting proper transport through the plasma membrane, resulting cell death. It has believed that the penetration of nanoparticle into the bacteria affecting loss via interaction with phosphorous and sulfur containing compounds for example DNA. The cellular proteins need denature and ability of replication becomes inactive when the nanoparticle penetrate the membrane. In addition, that Zr ions nanoparticles would be attractive between the positive and negative charge of nanoparticles inside microorganism cell membrane. Correspondingly, uncommon studies recommended that metal oxide inhibits microbial pathogens.

Table 1Inhibition zone (mm)

Samples	S.arueas 100-50-25%	E.coli 100-50-25%
2Fe	30-25-23	27-25-20
3Fe	30-25-20	30-23-20
4Ni	27-27-23	31-28-23
5Ni	25-27-20	30-30-20
Ciprofloxacin	35	40

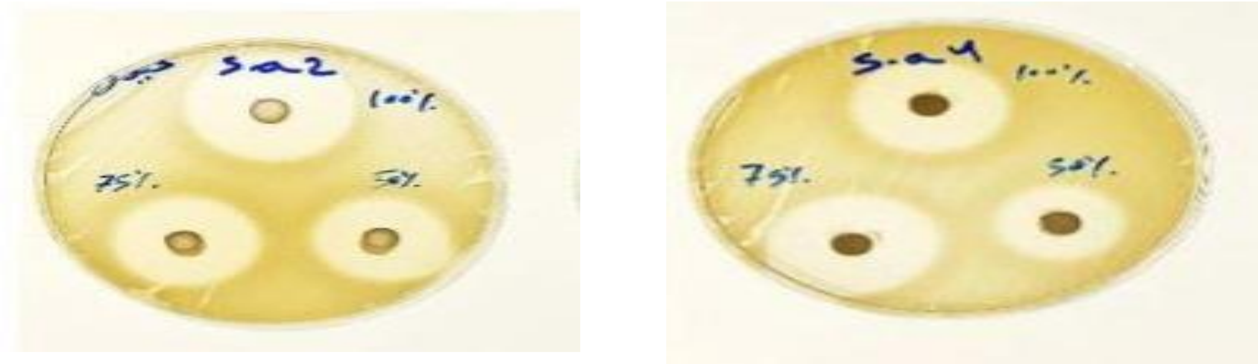

Figure 6 S.arueas ZrO2 with Fe and Ni prepared via atmospheric pressure plasma system jets

Figure 7 E.coli ZrO2 with Fe and Ni prepared via atmospheric pressure plasma system jets

Conclusions

This study provides to the evolving scene of nanomaterials by exploring the effects of Fe and Ni anode on ZrO2 nanopowders. The outcomes of this work hold ability for diverse applications, including advanced photocatalysis for environmental remediation, optoelectronic devices such as sensors and solar cells, and biomedical applications. The tailored properties of the ZrO2 nanocomposite are controlled to reveal innovative promises in engineering of materials and technology progress.

References

[1] Kozlovskiy, A. L., Zdorovets, M. V., & Uglov, V. V. (2024). Study of morphology, phase composition, optical properties, and thermal stability of ZrO_2 nanoparticles synthesized by hydrothermal method. Scientific Reports, 14(1), 80399.

[2] Raj, S., et al. (2023). A review of ZrO_2 nanoparticles applications and recent advancements. Ceramics International, 49(20), 32343–32358.
[3] American Elements. (n.d.). Zirconium Oxide (ZrO_2) Properties. Retrieved April 12, 2025.
[4] López, N., & González, J. (2005). Bulk and surface structures of iron doped zirconium oxide systems: Influence of preparation method. Journal of Materials Science, 40(4), 933–942.
[5] Dong H, Yang GJ, Cai HN, Ding H, Li CX, Li CJ. The influence of temperature gradient across YSZ on thermal cyclic lifetime of plasma-sprayed thermal barrier coatings. Ceram Int 2015;41:11046-56.
[6] Mücklich F, Ilić N. RuAl and its alloys. Part I. Structure physical properties, microstructure and processing. Intermetallics 2005;13:5-21.
[7] Mücklich F, Ilić N, Woll K. RuAl and its alloys, part II: mechanical properties, environmental resistance and applications. Intermetallics 2008;16:593–608.
[8] Iang, N., Ji, A., & Cao, Z. (2009). Atmospheric pressure plasma jet: Effect of electrode configuration, discharge behavior, and its formation mechanism. Journal of Applied Physics, 106(1), 013308.
[9] M. Chen, J. Zhang, T. Yang, Sh. Mao and H. Zhao, "Peroxymonosulfate activation for preferential generation of hydroxyl radical with atomic Mn anchored TiO2 in photoelectrochemical process", Environmental Functional Materials, 2023
[10] Kato, Y., Kagawa, M., & Syono, Y. (1998). Component distribution in plasma-deposited ultrafine powders of binary (Cr_2O_3, Fe_2O_3, SnO_2)–Al_2O_3 systems. Materials Letters, 35(3–4), 266–269.
[11] Wang Y, Guo HB, Peng H, Peng LQ, Gong SK. Diffusion barrier behaviors of (Ru,Ni)AI/NIAl coatings on Ni-based superalloy substrate. Intermetallics 2011;19:191-5.
[12] Ananth, A., & Mok, Y. S. (2015). Dielectric barrier discharge plasma-mediated synthesis of several oxide nanomaterials and its characterization. Powder Technology, 269, 259–266.
[13] A. A. Haidry, W. Yucheng, Q. Fatima, A. Raza, L. Zhong, H. Chen, C. R. Mandebvu and F. Ghani, "Synthesis and characterization of TiO2 nanomaterials for sensing environmental volatile compounds (VOCs): A review", TrAC Trends in Analytical Chemistry, 2024
[14] X. Wu, 'Applications of Titanium Dioxide Materials', Titanium Dioxide - Advances and Applications. Intech. Open, 2022
[15] Jiang, N., Ji, A., & Cao, Z. (2009). Atmospheric pressure plasma jet: Effect of electrode configuration, discharge behavior, and its formation mechanism. Journal of Applied Physics, 106(1), 013308.
[16] K. B. Riad, P.M. Wood-Adams and K. Wegner, "Flame-made TiO2 (B)", Materials Research Bulletin, 2018
[17] D. Chittinan, P. Buranasiri, T. Lertvanithpho, P. Eiamchai, K. Tantiwanichapan, A. Sathukarn, S. Limwichean, A. Klamchuen, T. Wutikhun, P. Limsuwan, H. Nakajima, W. Phae-ngam, N. Triamnak and M. Horprathum, "Tailoring the structural and optical properties of fabricated TiO2 thin films by O2 duty cycle in reactive gas-timing magnetron sputtering, Vacuum, 2023
[18] Z. Liu , Q. Chen, Z. Wang, L. Yang, and Ch. Wang, "Production of titanium dioxide powders by atmospheric pressure plasma jet", The Fourth International Conference on Surface and Interface Science and Engineering, Physics Procedia., 2011
[19] L. H. Nie, S. Shi, Y. Xu, Q. H. Wu and A. M. Zhu, "Plasma Process", Poly., 2007
[20] J. Ovenstone, "Preparation of novel titania photocatalysts with high activity", Journal of Materials Science, 2001
[21] Patel, S., Baker, N., Marques, I., & Shokuhfar, T. (2017). Transparent TiO_2 nanotubes on zirconia for biomedical applications. RSC Advances, 7(54), 33740–33747.
[22] Ramos-Justicia, J. F., Ballester-Andújar, J. L., Urbieta, A., & Fernández, P. (2023). Growth of Zr/ZrO_2 core-shell structures by fast thermal oxidation. arXiv.